MATHEMATICA MONTISNIGRI
Vol XLV (2019)

MODELING OF THERMAL CONDUCTIVITY OF SI IN THE RANGE FROM THE NORMAL TO NEAR-CRITICAL CONDITIONS

O.N. KOROLEVA[1,2*], M.M. DEMIN[1], V.I. MAZHUKIN[1,2], A.V. MAZHUKIN[1,2]

[1]Keldysh Institute of Applied Mathematics of RAS, Russia, Moscow

[2]National Research Nuclear University MEPhI, Russia, Moscow

* Corresponding author. E-mail: koroleva.on@mail.ru

DOI: 10.20948/mathmontis-2019-45-7

Summary. In a wide temperature range, including the semiconductor-metal phase transition region and the near-critical region, the results of modeling the silicon phonon thermal conductivity are presented. Since the transfer of thermal energy is carried out by phonons and free charge carriers, it is necessary to take into account both the contribution of phonons and electrons in the total thermal conductivity. In contrast to metals, heat transfer in silicon in the solid state is determined by phonon thermal conductivity. Although the contribution of the electronic component to the total thermal conductivity increases with increasing temperature, the inclusion of phonon thermal conductivity is of particular importance in liquid silicon. At higher temperatures, phonon thermal conductivity plays an important role in the modeling of the mechanisms of interaction of pulsed laser radiation with silicon in the framework of the two-temperature continuum model. Obtaining the temperature dependence of phonon thermal conductivity in such a wide temperature range from experiment is problematic. In this work, phonon thermal conductivity was obtained in the range $300 \leq T \leq 6500$ K from molecular dynamics simulation using the KIHS potential.

1 INTRODUCTION

Over the past decades, laser processing of silicon by short pulses has been developing rapidly. The possibility of introducing of a large amount of energy into a densely localized region through laser irradiation has been used in a large number of applications. Among them are such as the production of nanomaterials [1–4], surface nanostructuring [5, 6], chemical and physical synthesis [6–8]. Therefore, the fundamental mechanisms of the interaction of short-pulse laser radiation with a silicon target cause a long-term steady interest of researchers. A recognized tool for the theoretical study of laser interaction with a target is mathematical modeling. The problem of the adequacy and reliability of simulation results is associated with determining the properties of the target. The information on the temperature dependence of thermal conductivity is a necessary characteristic of a target when modeling laser heating of a substance using continuum models [9]. It is known that in accordance with the classical concepts, in a solid there are two mechanisms of heat transfer: elastic lattice vibrations and free electrons, therefore, thermal conductivity can be represented by lattice and electronic components. However, the contributions of phonon and electronic thermal conductivities at high temperatures are difficult to obtain from experiment. Therefore, in this work, the study of the thermal conductivity of the silicon lattice is carried out in the

2010 Mathematics Subject Classification: 82C26, 68U20, 74A15.
Key words and Phrases: Molecular Dynamics Simulation, Near-Critical Region, Phonon Thermal Conductivity of Silicon.

framework of the atomistic approach, which gives an understanding of the thermal behavior of silicon at the nanoscale.

Atomistic models are a system of differential equations that describes a set of interacting particles (atoms, ions, molecules). When using atomistic models to study various properties of substances, the most important role is played by the choice of the interaction potential between the particles, since the reliability of the results obtained directly depends on it.

The construction of the interatomic interaction potential for silicon has a number of features and is more complicated than for metals. Therefore, in order to determine the applicability of the selected interaction potentials in certain particular conditions, careful test calculations are required. This problem is especially acute in materials with covalent bonds, which include silicon. In [10], based on a comparison of the interaction potentials, it was found that the most suitable for modeling silicon are the Stillinger – Weber potentials (SW) and KIHS [11-13]. In this study, the KIHS potential was used to simulate the phonon thermal conductivity of silicon.

The thermal conductivity of phonons of single-crystal silicon was simulated over a wide range of temperature values using the widespread LAMMPS (Large-scale Atomic/Molecular Massively Parallel Simulator) application package [14]. It implements support for many pair and many-particle short-range potentials, it is possible to write atomic configurations to a text file, and thermostats and barostats are built-in. The computational algorithm is based on the Verlet finite-difference scheme [15]. The velocity and pressure for the ensemble of particles were adjusted using a thermostat and a Berendsen barostat [16].

The determination of phonon thermal conductivity in the framework of classical molecular dynamics is a complex problem. Despite the fact that research on the theoretical determination of the thermal conductivity of a silicon lattice has been going on for several decades, it has not been possible to obtain the temperature dependence in a wide range necessary for mathematical modeling, which confirms the complexity of the problem. The results of modeling the phonon thermal conductivity of silicon, as a rule, contain values at one, two, or three temperatures [17–21], either a temperature dependence, but only for the solid phase [22–28], or a narrow range dependence near the melting point [29].

The most common methods for calculating thermal conductivity are the direct method “heat source - sink” [17, 30, 31] and the Green-Kubo method [17, 30, 32]. The direct method is nonequilibrium, it is based on the application of a temperature gradient on the modeling cell, and therefore is similar to the experimental situation. The Green-Kubo method is equilibrium; it uses current fluctuations to calculate the thermal conductivity using the fluctuation-dissipation theorem [33]. Thermal conductivity, according to the Green-Kubo method, can be expressed through the autocorrelation function of the microscopic heat flux. A detailed analysis of the use of both methods for calculating the phonon thermal conductivity of silicon was carried out in [17]. One of the advantages of the direct method, in comparison with the Green-Kubo method, is the saving of computational resources, which is very important, sometimes determining for choosing a modeling method. For example, as noted in [17], for a direct method, a simulation time of 1 ns is sufficient to obtain a smooth temperature profile, and the value of κ converges to within ± 10%, the same simulation time using the Green-Kubo method leads to statistical errors up to ± 50%. Both methods demonstrate the effects of finite size. These effects arise if the mean free path of phonons is comparable to the size of the simulation cell. For a system such as Si, the required size of the computational domain to achieve a completely convergent value of κ may be beyond the

reach of atomistic modeling. Finite size effects impose a restriction on the smallest length of the computational domain. The thermal conductivity of silicon can be obtained by a direct method from modeling systems of different sizes and extrapolating the results to a system of infinite size. The equilibrium Green-Kubo method, in comparison with the direct method, has an advantage for calculating the thermal conductivity of highly anisotropic materials [30].

The Evans method [34, 35] is characterized by the combination of the elements of the equilibrium (Green-Kubo) and nonequilibrium perturbation method developed in [36.37]. Like the direct method, the Evans method reduces the computational time required to obtain the phonon thermal conductivity. Like the Green-Kubo method, this method is well suited only to describe the properties of homogeneous systems.

Along with classical molecular dynamics, the ab-initio approach [19, 22], the method of lattice dynamics and molecular dynamics based on the solution of the Boltzmann equation [38, 39], are also used to determine phonon thermal conductivity.

In this paper, the direct method (DM) was chosen as the most simple and economical from a computational point of view as an approach to determining the temperature dependence of the phonon thermal conductivity of silicon using molecular dynamics (MD).

The aim of this work is to obtain the temperature dependence of phonon thermal conductivity in the range from normal conditions to the critical region using the KIHS potential [11–13] in the framework of the DM of molecular dynamics modeling. The obtained temperature dependence of phonon thermal conductivity is planned to be used in the continuum simulation of laser evaporation of silicon.

2 STATEMENT OF THE PROBLEM. COMPUTATIONAL ALGORITHM.

To determine the thermal conductivity of the phonon subsystem of silicon, a series of calculations was performed based on molecular dynamics models. The phonon thermal conductivity was determined on the basis of the DM.

DM is a method of nonequilibrium molecular dynamics (NEMD), where regions of a heat source and sink are created in a modeling cell to apply a constant heat flux along the direction of interest. The thermal conductivity κ_{lat} is determined by the known heat flux according to the Fourier law [40]

$$W = -\kappa_{lat} \frac{\partial T}{\partial x} \tag{1}$$

where W is the heat flux, x is the coordinate in the direction of flux. The difficulty in applying the direct method to solids lies in the fact that the size of the modeling region should be much larger than the mean free path of phonons in a substance. For a crystal, this is difficult to do, because requires a very large size of the computational domain and, accordingly, a very large number of atoms. For example, 500 million atoms were used in [41]. Therefore, when calculating with a small number of atoms, the thermal conductivity coefficient turns out to be dependent on the length of the region due to phonon scattering at the boundary. Therefore, to limit the size of the simulation cell and make the simulation feasible, you can use the scaling procedure in which thermal conductivity is determined for several lengths of the simulation cell along the x direction. Then, the inverse dependence of the thermal conductivity $1/\kappa_{lat}$ is constructed with respect to the inverse value of the length of the simulation cell, 1/L, and the thermal conductivity is determined by extrapolating the data $1/L \to 0$ [17]. Such a procedure

is justified by the expression for thermal conductivity obtained from the kinetic theory [17, 31]. Another disadvantage of the direct method is that the temperature gradient must be large in order to reduce the influence of temperature fluctuations. Also, the average temperature is reached only in the middle of the region, and the rest of the region is at a temperature different from the average value.

The simulation domain in the form of a parallelepiped with sizes of 10×10×20 unit cells (lattice constant 0.543 nm) with periodic boundary conditions along three axes was considered. As the interaction potential, the KIHS potential is used [13]. The region along the x axis was divided into 20 intervals, and heating is performed in the first interval, and the heat sink is in the 11th. At each time step, a fixed amount of heat dQ_N was pumped into the heating region, and the same amount was taken from the sink region. The heat flux W was calculated as

$$W = dQ/(SNdt)/2, \quad (2)$$

where $dQ = N \times dt \times \delta Q_N$ is the total energy released, where δQ_N is the energy released in 1 time step, N is the number of time steps, dt is the time step size, S is the cross-sectional area of the region. Division by 2 is used due to periodic boundary conditions, i.e. heat distribution goes in 2 directions. Then, the resulting temperature gradient was calculated, and the Fourier law (1) was used to obtain thermal conductivity. The choice of time step depended on temperature, and took the values from 3 fs at 300K to 1 fs at 4000K and higher.

3 MODELING RESULTS

Fig. 1 shows the time-averaged spatial temperature profile used to calculate the thermal conductivity. The average temperature is 1690 K. In a small region (~ 8 nm), a very nonlinear temperature profile is observed in the immediate vicinity of the source. The same strongly nonlinear temperature profile is also observed near the sink. In the intermediate region, the temperature profile is close to a linear dependence. This gap between the heat source and the heat sink is indicated on the graph (Fig. 1) by dashed lines. In this interval, a temperature gradient was measured. The presence of a heat source and heat sink and the use of periodic boundary conditions create a current in two opposite directions. Since the heat flux passes along a clearly defined direction in the lattice, a single simulation can be used to obtain thermal conductivity along only one direction of the crystal lattice. Therefore, the heat flux was determined by a series of calculations. For the crystal, calculations were carried out for 5 different sizes of the region from 20 to 320 unit cells with a constant cross section of 10×10 cells. The maximum number of atoms was 256,000.

The heat flux (2) was determined from the temperature difference between the heating and heat sink areas, for which the instantaneous temperature difference was averaged over the entire calculation time after establishing the stationary distribution. To increase the accuracy of the calculations, the temperature difference was calculated not over the entire interval between the source and the sink, but in its central part with a length of 0.8 of the full length. The calculation time varied from 480 ps for a temperature of 350 K to 3.8 ns at 1550 K and a higher temperature.

To calculate the thermal conductivity from the Fourier law (1), the scaling procedure described above was used. The inverse dependence of the thermal conductivity $1/\kappa_{lat}$ was constructed with respect to the reciprocal of the length of the simulation cell 1/L, and the

thermal conductivity was determined by extrapolating the data 1/L → 0. For the liquid state, only one calculation was performed for a size of 40 cells, for large sizes the results were approximately the same. Fig. 2 shows the dependences of the reciprocal of the thermal conductivity on the reciprocal of the size of the region for two temperatures 350 K and 1550 K.

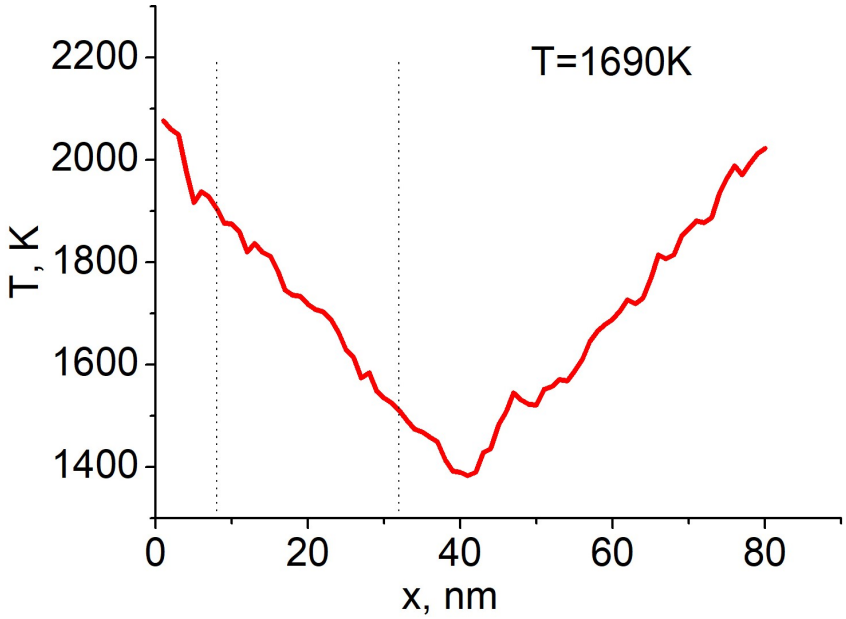

Fig. 1. Spatial profile of the temperature at one of the time instants.

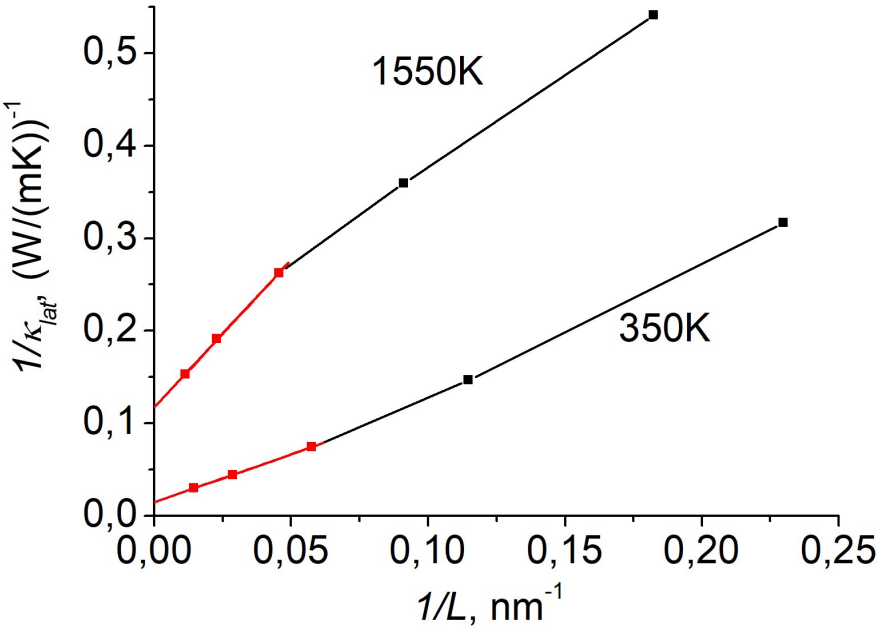

Fig. 2. Dependence of the reciprocal of the thermal conductivity on the reciprocal of the size of the region for two temperatures.

The results of calculations on the graph are shown by red lines and markers. Extrapolation was performed using the least squares method at the three points corresponding to the longest lengths of the region (red lines and markers in Fig. 2).

Fig. 3 shows the obtained temperature dependence of the phonon thermal conductivity with the experimental data [42] and the data from [29] for the Stillinger – Weber potential, as well as a theoretical estimate [44, 45]. The dashed line shows the extrapolation of the phonon thermal conductivity to the critical point. In this work, we used the silicon critical point parameters T_{crit} = 6750±250 K, ρ_{crit} = 0.24±0.06 g/cm^3, P_{crit} = 800±300 bar obtained from molecular dynamics modeling with the KIHS potential in [43].

According to theoretical concepts [45], the thermal conductivity of the lattice of crystalline silicon is calculated as follows

$$\kappa_{lat}(T) = \frac{1}{3} c_v \rho \omega_F \bar{l}_F \qquad (3)$$

where ω_F is the velocity of sound, or the group velocity of thermal vibrations of phonons; $\bar{l}_F$ is the average mean free path of elastic waves - phonons; c_v is the specific heat of the lattice, ρ is the density. Figure 7 shows the approximation of the theoretical estimate (blue line) obtained in [44]

$$\kappa_{lat}(T) = 15{,}85 \times T_{lat}^{-1.23} \text{ W/mK}$$

Phonon thermal conductivity is difficult to obtain from experiment, therefore, experimental data are given for the total thermal conductivity of silicon.

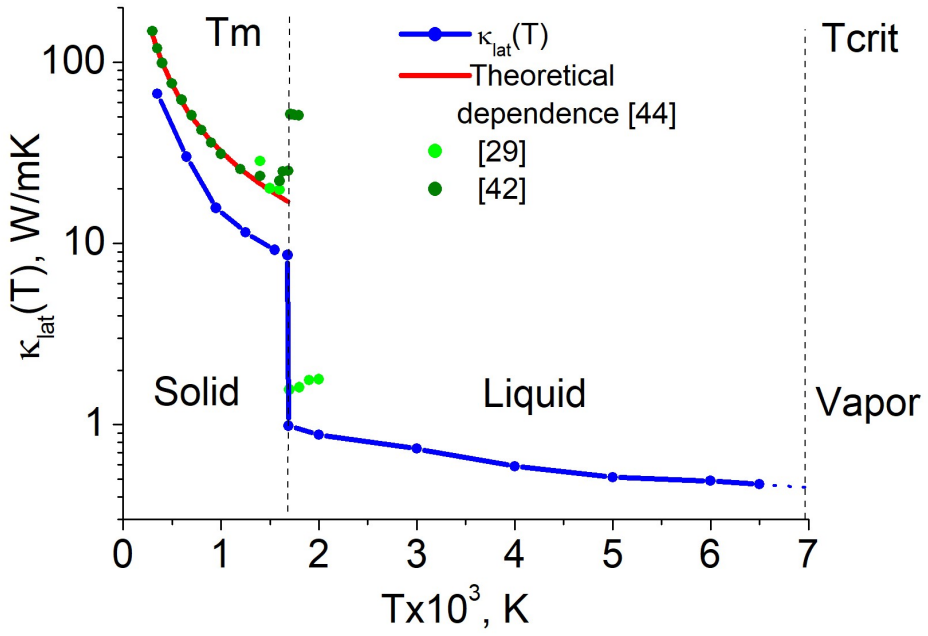

Fig. 3. Temperature dependence of the phonon thermal conductivity of silicon (this work), experimental data for total thermal conductivity [42], and data from [29] for the Stillinger-Weber potential. A theoretical estimate for the solid phase is also given [44].

In crystalline silicon, phonon thermal conductivity is decisive. The difference between the calculation data with the KIHS potential and the experimental values of the total thermal conductivity is approximately 60% at 350K. At the melting temperature, the difference from experiment doubles, which is explained by an increase in the contribution of electronic thermal conductivity to the total thermal conductivity. A comparison of the results of calculations with a theoretical estimate [44, 45] shows a qualitative coincidence.

At the semiconductor-metal phase transition, the phonon thermal conductivity decreases stepwise, which is explained by the destruction of long-range bonds. At the equilibrium melting temperature T_m = 1687 K, the jumps in the phonon thermal conductivity of silicon is 88.9%. In the calculation of thermal conductivity with the Stillinger – Weber potential [29], the jump estimate is 92.08%.

After melting, silicon from a semiconductor becomes a metal, because of which the electronic component in the thermal conductivity becomes decisive [46, 47], and the phonon component differs significantly from the experimental data on total thermal conductivity.

The difference between the phonon thermal conductivity in the liquid of the potentials KIHS and SW [29] is 60%. At a temperature of 2000 K, the difference between the results obtained in this work and the data obtained using the ab-initio approach from [19] is 30.8% (0.91 and 0.63 W/(mK), respectively).

At the temperature $T > 5000$ K, phonon thermal conductivity tends to decrease, which does not contradict theoretical concepts. In the near-critical region, the phonon thermal conductivity obtained from the simulation results is approximately 0.47 W/(mK) at T = 6500K, approximately the same value at temperature $T \approx T_{crit}$ (0,45 W/(mK)).

4. CONCLUSION

1. Based on a series of calculations by the direct method using molecular dynamics modeling, the temperature dependence of the phonon thermal conductivity of silicon was obtained in the temperature range 300 <T <6500 K. The KIHS potential was used in the simulation.

2. Comparison of the simulation results with the KIHS potential (this work) with the simulation results with the Stillinger – Weber potential [29] showed that for high-temperature processes ($T_m < T < T_{crit}$) in silicon, the best results are achieved when the KIHS potential is used, in contrast to low-temperature processes ($T \le T_m$), where the classic Stillinger –Weber potential has an advantage.

3. Comparison of the results obtained at a temperature T = 2000K with the results obtained using the ab-initio approach [19] showed a slight discrepancy of 30.8% (0.91 and 0.63 W/(mK), respectively).

4. Comparison of the results of modeling of the phonon thermal conductivity with the experimental values of total thermal conductivity [42] makes sense only in crystalline silicon in the range 300 K $< T <$ 1000 K, since at a temperature above $T >$ 1000 K the degeneracy of charge carriers increases, the band gap decreases, which leads to a rapid increase in the concentration of carriers and, accordingly, to an increase in the thermal conductivity of electrons [46, 47]. The difference between the phonon thermal conductivity and the total thermal conductivity with increasing temperature will only increase, especially after a phase transition in liquid silicon. After melting at the equilibrium melting temperature T_m = 1687 K from the side of the solid phase, the phonon thermal conductivity obtained from molecular

dynamic modeling (MDM) is 2.9 times less than the experimental data and theoretical estimate. From the side of the liquid phase, the phonon thermal conductivity obtained from MDM is ~ 50 times lower than the experimental values of the total thermal conductivity.

5. In the near-critical temperature range of $5000\,\mathrm{K} < T < T_{crit}$, the phonon thermal conductivity decreases, which does not contradict theoretical concepts, and at $T \approx T_{crit}$ its value is approximately $\kappa_{lat} \approx 0.45$ W/(mK).

REFERENCES

1. Urs Zywietz, Andrey B. Evlyukhin, Carsten Reinhardt & Boris N. Chichkov, "Laser printing of silicon nanoparticles with resonant optical electric and magnetic responses", *Nat. Comm*., **5**, 3402 (2014).
2. Urs Zywietz, Mikolaj K. Schmidt, Andrey B. Evlyukhin, Carsten Reinhardt, Javier Aizpurua, and Boris N. Chichkov, "Electromagnetic Resonances of Silicon Nanoparticle Dimers in the Visible", *ACS Photonics*, **2** (7), 913–920 (2015).
3. Boris Chichkov, Urs Zywietz and Lothar Koch. "Laser printing of silicon nanoparticles and living cells", *Biomedical Optics & Medical Imaging, Proc. SPIE Int. Soc. Opt. Eng.*, (2015).
4. M E Shaheen, J E Gagnon and B J Fryer, "Femtosecond laser ablation behavior of gold, crystalline silicon, and fused silica: a comparative study", *Las. Phys*., **24,** 106102(1-8) (2014).
5. Vinod Parmar, Yung C. Shin, "Wideband anti-reflective silicon surface structures fabricated by femtosecond laser texturing", *Appl. Sur. Sci.*, **459**, 86-91 (2018).
6. Benjamin Franta, Eric Mazur and S. K. Sundaram, "Ultrafast laser processing of silicon for photovoltaics", *Int. Mater. Rev.*, **63**(4), 227-240 (2018).
7. A. Al-Kattan, Y.V. Ryabchikov, T. Baati, V. Chirvony, J. F. Sánchez-Royo, M. Sentis, D. Braguer, V.Yu. Timoshenko, M. Anne Esteve, A.V. Kabashin, "Ultrapure laser-synthesized Si nanoparticles with variable oxidation states for biomedical applications", ***J. Mater. Chem. B*****, 4,** 7852-7858 (2016).
8. R.F. Balderas-Valadez, J.O. Estévez-Espinoza, U. Salazar-Kuri, C. Pacholski, W.L. Mochan, V. Agarwal, "Fabrication of ordered tubular porous silicon structures by colloidal lithography and metal assisted chemical etching: SERS performance of 2D porous silicon structures", *Appl. Sur. Sci.*, **462**, 783-790 (2018).
9. V. I. Mazhukin, A. V. Mazhukin, M. M. Demin, A. V. Shapranov, "Nanosecond laser ablation of target Al in a gaseous medium: explosive boiling", *Applied Physics A: Material Science and Processing*, **124** (3), 237(1-10), (2018).
10. V.I. Mazhukin, A.V. Shapranov, A.V. Rudenko, "Comparative analysis of potentials of interatomic interaction for crystalline silicon", *Math. Montis.*, **30**, 56-75 (2014).
11. F.H. Stillinger, T.A. Weber, "Computer simulation of local order in condensed phases of silicon", *Phys. Rev. B*, **31**, 5262-5271 (1985).
12. L. Pizzagalli, J. Godet, J. Guenole, S. Brochard, E. Holmstrom, K. Nordlung, T. Albaret, "A new parametrization of the Stillinger-Weber potential for an improved description of defects and plasticity of silicon", *J. Phys, Condens. Matter*, **25**, 055801(1-12) (2013).
13. T. Kumagai, S. Izumi, S. Hara, S. Sakai, "Development of bond-order potentials that can reproduce the elastic constants and melting point of silicon for classical molecular dynamics simulation", *Comp. Mater. Sci.*, **39** (2), 457-464 (2007).
14. Lammps project website: http://lammps.sandia.gov/ (accessed July 7, 2019).
15. L. Verlet, "Computer "Experiments" on Classical Fluids. I. Thermodynamically Properties of Lennard-Jones Molecules", *Phys. Rev.*, **159**, 98-103 (1967).
16. H.J.C. Berendsen, J.P.M. Postma, W.F. Van Gunsteren, A. DiNola, J.R. Haak, "Molecular dynamics with coupling to an external bath", *J. Chem. Phys.*, **81**, 3684-3690 (1984).

17. P. K. Schelling, S. R. Phillpot, P. Keblinski, "Comparison of atomic-level simulation methods for computing thermal conductivity", *Phys. Rev. B*, **65**, 144306 (2002)
18. Wang Zenghui, Li Zhixin, "Lattice dynamics analysis of thermal conductivity in silicon nanoscale film Lattice dynamics analysis of thermal conductivity in silicon nanoscale film*", Applied Thermal Engineering*, **26**, 2063–2066 (2006)
19. Jun Kang and Lin-Wang Wang, "First-principles Green-Kubo method for thermal conductivity calculations", *Phys. Rev. B*, **96**, 020302(R) (2017)
20. Yongjin Lee and Gyeong S. Hwang, "Force-matching-based parameterization of the Stillinger-Weber potential for thermal conduction in silicon", *Phys. Rev. B*, **85**, 125204 (2012)
21. D. P. Sellan, E. S. Landry, J. E. Turney, A. J. H. McGaughey, and C. H. Amon, "Size effects in molecular dynamics thermal conductivity predictions", *Phys. Rev. B*, **81**, 214305 (2010)
22. Christian Carbogno, Rampi Ramprasad, and Matthias Scheffler, "Ab Initio Green-Kubo Approach for the Thermal Conductivity of Solids", Phys. Rev. Lett., **118**, 175901 (2017).
23. Sebastian G. Volz, Gang Chen, "Molecular-dynamics simulation of thermal conductivity of silicon crystals", *Phys. Rev. B*, **61**(4), 2651-2656 (2010)
24. Keivan Esfarjani and Gang Chen, *Heat transport in silicon from first principles calculations*, arXiv: 1107.5288v1, (2011)
25. Shenghong Ju and Xingang Liang, "Thermal conductivity of nanocrystalline silicon by direct molecular dynamics simulation", *J. Appl. Phys*., **112**, 064305 (2012)
26. D. A. Broido, M. Malorny, G. Birner, Natalio Mingo, D. A. Stewart, "Intrinsic lattice thermal conductivity of semiconductors from first principles", *Appl. Phys. Lett*., **91**, 231922 (2007)
27. Lin Sun, Jayathi Y. Murthy, "Molecular dynamics simulation of phonon transport in EDIP silicon", *Proceedings of HT2005, San Francisco, California, USA*, 1-6 (2005)
28. P.C. Howell, "Comparison of molecular dynamics methods and interatomic potentials for calculating the thermal conductivity of silicon", *J. Chem. Phys*., **137**, 224111 (2012).
29. C. H. Baker, C. Wu, R. N. Salaway, L. V. Zhigilei, P. M. Norris, "Resolving the vibrational and electronic contributions to thermal conductivity of silicon near the solid-liquid transition: molecular dynamics study", *I. J. Trans. Phenomena*, **13**, 143–150 (2013)
30. L. Hu, W. J. Evans, P. Keblinski, "One-dimensional phonon effects in direct molecular dynamics method for thermal conductivity determination", *J. Appl. Phys*., **110**, 113511 (2011)
31. Florian Müller-Plathe, "A simple nonequilibrium molecular dynamics method for calculating the thermal conductivity", *J. Chem. Phys.*, **106**, 6082 (1997).
32. R. Zwanzig, "Time-correlation functions and transport coefficients in statistical mechanics", *Annu. Rev. Phys. Chem*., **16,** 67-102 (1965).
33. R Kubo, "The fluctuation-dissipation theorem", *Rep. Prog. Phys.*, **29,** 255-284 (1966)
34. Denis J. Evans, "Homogeneous nemd algorithm for thermal conductivity - application of non-canonical linear response theory", *J. Phys. Lett.,* **91A**(9), 457-460 (1982).
35. Kranthi K. Mandadapu, Reese E. Jones, Panayiotis Papadopoulos, "A homogeneous non-equilibrium molecular dynamics method for calculating thermal conductivity with a three-body potential", *J. Chem. Phys.*, **130** (20), 204106(1-18) (2009).

36. G. Ciccotti, G. Jacucci and I.R. McDonald, "Thermal response to a weak external field", *J. Phys.* C: *Solid State Phys.,* **11** (13)**,** 1509-1513 (1978).
37. G. Ciccotti, G. Jacucci, and I.R. McDonald, "Thought experiments by molecular dynamics", *J. Stat. Phys*., **21**, 1–22 (1979).
38. J. E. Turney, E. S. Landry, A. J. H. McGaughey, and C. H. Amon, "Predicting phonon properties and thermal conductivity from anharmonic lattice dynamics calculations and molecular dynamics simulations", *Phys. Rev. B*, **79**, 064301 (2009).
39. A. J. H. McGaughey and M. Kaviany, "Quantitative validation of the Boltzmann transport equation phonon thermal conductivity model under the single-mode relaxation time approximation", *Phys. Rev. B*, **69**, 094303 (2004).
40. W. Evans and P. Keblinski, "Thermal conductivity of carbon nanotube cross-bar structures", *Nanotechnology,* **21**(47), 475704, (2010) doi: 10.1088/0957-4484/21/47/475704
41. Chaofeng Hou, Ji Xu, Wei Ge and Jinghai Li, **"**Molecular dynamics simulation overcoming the finite size effects of thermal conductivity of bulk silicon and silicon nanowires**",** *Modelling Simul. Mater. Sci. Eng*., **24,** 045005 (1-9) (2016)
42. Eiji Yamasue, Masahiro Susa, Hiroyuki Fukuyama, Kazuhiro Nagata, "Thermal conductivities of silicon and germanium in solid and liquid states measured by non-stationary hot wire method with silica coated probe", *Journal of Crystal Growth,* **234,** 121–131 (2002).
43. V.I. Mazhukin, A.V. Shapranov, O.N. Koroleva, A.V. Rudenko. Molecular dynamics simulation of critical point parameters for silicon, *Math. Montis*., **31**, 56-76 (2014).
44. H.M. Van Driel, "Kinetics of high-density plasmas generated in Si by 1.06- and 0.53-mm picosecond laser pulses", *Phys. Rev. B*, **35,** 8166 – 8176 (1987).
45. W. Neil, N. Ashcroft, D. Mermin, *Solid state physics*, Saunders College, Vol. 1, 1976.
46. O.N. Koroleva, A.V. Mazhukin, "Determination of thermal conductivity and heat capacity of silicon electron gas", *Math. Montis*., **40**, 99-109 (2017)
47. O.N. Koroleva, A.V. Mazhukin, V.I. Mazhukin, "Modeling of silicon characteristics in the semiconductor-metal phase transition region", *Math. Montis.*, **41**, 73-90 (2018).

Received May 25, 2019